

AN EXPERIMENTAL STUDY ON ENERGY ABSORPTION CAPACITY OF COLUMNS IN REINFORCED CONCRETE STRUCTURES*

*By Tomonori OHNO** and Takashi NISHIOKA****

A number of experimental research works on the strength and ductility capacity of structures have been carried out in the past, which showed that the ductility capacity was strongly affected by loading condition. As far as such a repeated loading as earthquake motion is concerned, the design based on ductility factor is not always reasonable. The authors have proposed that the energy absorption capacity of structures is well-suited index for seismic safety. The purpose of this study is to investigate the energy absorption capacity of structures quantitatively. A series of five reinforced concrete columns were tested under four types of repeated loading. The results developed in this paper is intended to use in estimation of seismic safety.

1. INTRODUCTION

It is generally admitted that the deformation capacity of structures in itself is commonly evaluated by their ductility factor. It is a good index for earthquake resistant capacity in order to deal with the behavior of structures in such a strong earthquake motion that causes structures to collapse. Therefore, the most research works in the past on earthquake resistance of structures in civil engineering field are concerned with the variation of the resistant strength and deformation after yielding in the main members and connections of structures^{1)~15)}.

In general, the factors affecting on the strength and ductility of structures are several member constants (axial reinforcement ratio, ratio of hoop ties and shear-span ratio etc.), axial load and loading condition (loading rate, the number of loading cycles and the type of loading etc.). According to the past research works which dealt with these factors, it is pointed out that the reduction of deformation capacity is strongly affected by the number of repeated loading cycles and the increase of axial reinforcement ratio. Especially, the number of repeated loading cycles affects so greatly that the ductility reduces to about one half of the case in one directional loading^{2),15)}. Since the ductility factor which is widely used as an index of structural safety is varied under the influence of loading condition, it is not always reasonable to use it in earthquake resistant design. In the most research works which used equivalent linearized method to analyze elasto-plastic structures for earthquakes, the equivalent damping constant h_{eq} calculated from each cycle of hysteresis loop under repeated loading is adopted as an energy absorption capacity of structures^{15),19)~21)}. When the load-displacement loops of members under repeated loading is obtained both in experiment and

* partly presented at the 38th annual meeting conference of JSCE

** Member of JSCE, Reserch Fellow, University of Tsukuba (Niihari-gun, Ibaraki).

*** Member of JSCE, Dr. Eng., Associate Professor, Universtiy of Tsukuba (Niihari-gun, Ibaraki).

theoretical analysis, the area of hysteresis loop in one cycle is evaluated as equivalent to the viscous damping dissipated in the structural system.

On the other hand, the authors define in this paper the energy absorption capacity of members as the amount of absorbed energy up to its ultimate condition. We have been studying that the energy absorption capacity up to the ultimate state of structures is the most suitable index in structural response against earthquake motion¹⁶⁾⁻¹⁸⁾.

There are several research works which discuss the structural response under strong earthquake motion by energy concept. Akiyama²²⁾ and Suzuki et al.^{23),24)} discuss the energy absorption capacity of steel structures and gave the energy absorption capacity in relation to the plastic deformation capacity defined by several constants of members. There are very few research works on the energy absorption capacity of reinforced concrete structures. Only Okada et al.²⁵⁾ studied the relation between the energy dissipation and the plastic rotation capacity of reinforced concrete beams having various reinforcement ratios.

It is considered that the structural safety against strong earthquakes is estimated by comparing the energy absorption capacity of structures with the input energy imparted by earthquakes^{16),17)}. In this study, the energy absorption capacity in the flexural failure of reinforced concrete columns under repeated loading was investigated experimentally. The effect of loading cycles on the energy absorption capacity of reinforced concrete columns was measured quantitatively in different loading cycles and loading types. Since the number of loading cycles influenced on the response of actual structures beyond yield displacement was limited even in strong earthquake motion, it was chosen up to several tens of cycles in the experiment.

2. EXPERIMENTAL PROCEDURES

(1) Test Specimens

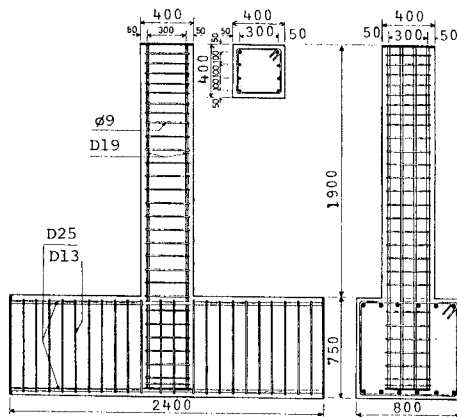


Fig.1 Configuration and dimension of RC column specimen.

Table 1 Details of test specimens and testing condition.

Specimen	Ratio of Axial Reinforcement (%)	Interval of Ties (cm)	Ratio of Ties (%)	Shear-Span Ratio	Axial Unit Stress (MPa)	Loading Types
NO.1	0.82	10	0.32	4.0	0.98	L-1
NO.2						L-2
NO.3						L-3
NO.4						L-3
NO.5						L-4

Fig.1 shows the configuration and dimensions of reinforced concrete column, which was modeled after the actual reinforced concrete piers of highway bridges having shear-span ratio about 4. Table 1 shows the details of test specimens and testing condition. Five test specimens were made all in the

Table 2 Mechanical properties of reinforcing bars.

Reinforcing Bar	Yield Strength (MPa)	Tensile Strength (MPa)	Extensibility (%)	Yield Strain ($\times 10^{-6}$)
SD30 D19	362	535	22.7	2072
SR24 $\phi 9$	325	449	21.7	1875

Table 3 Material of concrete.

Classification	Kind	Source	Specific Gravity	Fineness Modulus
Fine Aggregate	Sea Sand	KASHIMA	2.60	2.70
Coarse Aggregate	River Gravel	KINUGAWA	2.60	6.90

Table 4 Mix proportion.

Max. Size of Course Aggr. (mm)	Slump (cm)	Water-Cement Ratio W/C (%)	Sand-Aggr. Ratio S/a (%)	Unit Weight (Kg/m ³)			
				Cement	Water	Sand	Course Aggr.
25	8	54	39.5	258	139	760	1163

same dimension. The column was reinforced by deformed reinforcing bars D 19 (SD 30) and confined by hoop bars ϕ 9 (SR 24) at the spacing of 100 mm. Reinforcement ratio was 0.82% in axial reinforcing bar and 0.32% in hoop ties. The footing was designed as big as possible and stirrups were densely spaced to prevent the shear failure in footing. The footing section was strengthened also by the prestressing bars which were passed through the footing at both ends so that the failure due to shear cracks was prevented. The mechanical properties of reinforcing bars and the material properties of concrete are given in Table 2 and Table 3. The mix proportion of concrete and the designed slump are given in Table 4. The average compressive strength of concrete using 6 cylindrical specimens was 24.8 MPa.

(2) Loading Program

Fig.2 shows the general view of the testing machine and the test specimen set on the steel bed. The test specimen was fixed to the steel bed by 12 steel bars of 20 mm in diameter. Loads were applied vertically and laterally at the top of column by two electro-hydraulic servo actuators (the maximum capacity of 980 KN and the maximum stroke of ± 150 mm). Horizontal load was applied both in forward and backward directions under constant vertical axial load. Fig.3 shows four different loading types which were used in this experiment to investigate the effect of loading cycles on the energy absorption capacity. Of all loading types, L-1 was each one repetition of the relatively large amplitudes having $5 \delta_y$ and $8 \delta_y$ (δ_y is a measured horizontal displacement at yielding point). L-2 was each one repetition with increasing amplitudes from $1 \delta_y$ to $8 \delta_y$. L-3 and L-4 were each 5 and 10 repetitions under constant amplitudes of $2 \delta_y$, $3 \delta_y$, ..., respectively. Axial compressive force was set 127 KN in case of L-1, L-2, L-3 and L-5, and 314 KN in case of L-4, which corresponded to 0.98 and 1.96 MPa in compressive stress. The horizontal repeated load was applied by the actuator fixed to the reaction wall at the height of 160 cm from the bottom of the column. The test was

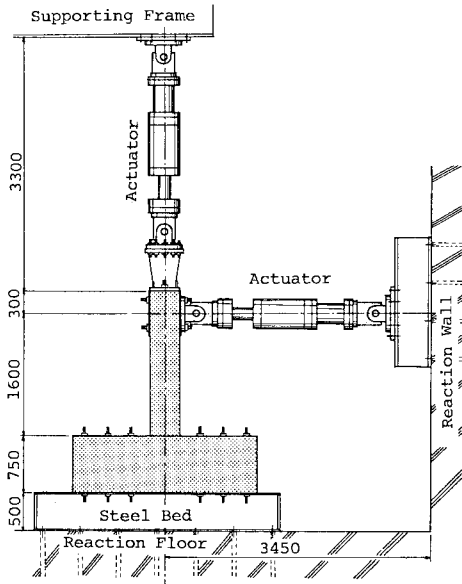


Fig.2 General view of testing machine and test specimen set on steel bed.

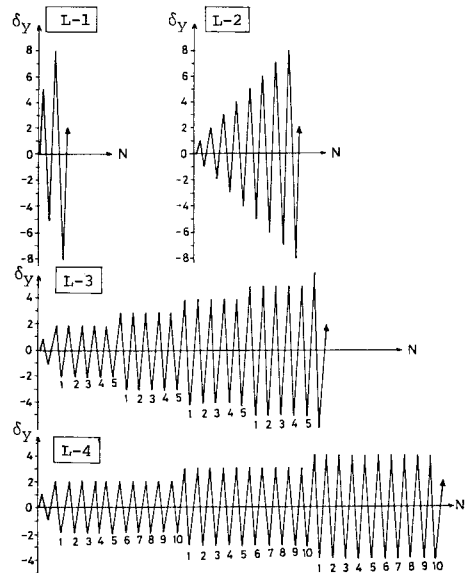


Fig.3 Various types of repeated loading.

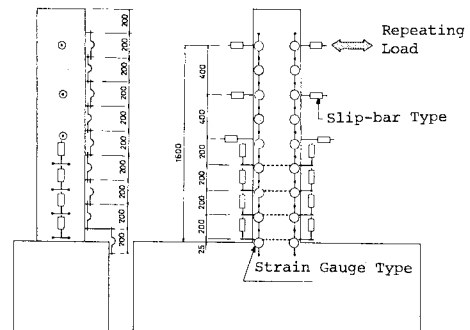


Fig.4 Measuring instruments and their positions.

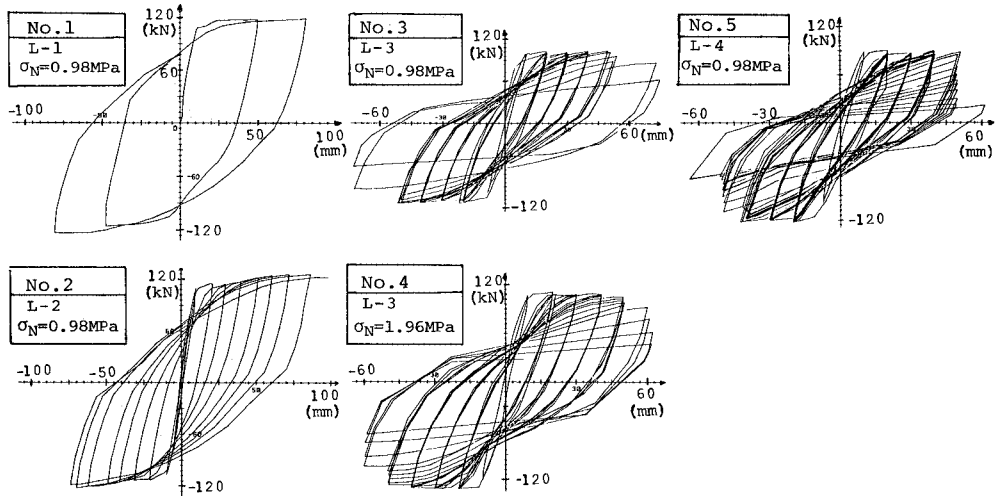


Fig.5 Load-displacement hysteresis loops at the top of column in various loading condition.

finished at the time when it was too dangerous to continue the experiment because of the serious failure in specimen.

(3) Measuring System

Measuring instruments and their positions are shown in Fig.4. The strain gauge type electric displacement meters (1/1000 mm in accuracy) and the slip-bar type electric resistant displacement meters (1/100 mm in accuracy) were used to measure horizontal displacement of the column. These meters were set on the column at the points 1, 3/4 and 2/4 of the column length from its bottom to the top. The same electric displacement meters were used to measure the change of rotation angle near the foot of column after cracking, which were set on the height of 25, 225, 425 and 625 mm from the foot. The curvature of column was measured with the strain gauge type electric displacement meters. These were placed at 20 cm intervals from the foot to the loading point. The strain in the axial reinforcing bars was measured by electric resistant strain gauges attached at twelve locations on both compression and tension side. Electric resistant strain gauges were also attached at five hoop ties within the range of 50 cm in height from the foot to observe hoop steel strain due to confinement of concrete and shear stress. The output of these measuring instruments was recorded into a cassette type magnetic tape by way of a micro computer at each loading step. At the same time the value of load and displacement at the loading point was displayed on a CRT and the relation between load and displacement was drawn on a X-Y plotter at each loading step to control the experiment. The deviation of axial and horizontal load from true values, which was due to increasing horizontal displacement in column, was modified automatically by computer program.

3. EXPERIMENTAL RESULTS

(1) Load-displacement Relationship

Fig.5 shows the load-displacement hysteresis loops in various loading types from the beginning to the end of the experiment. These loops show generally same features except the specimen No.1. It is clear that the stiffness is degraded after each reverse loading as the number of cycles increases. The enve-

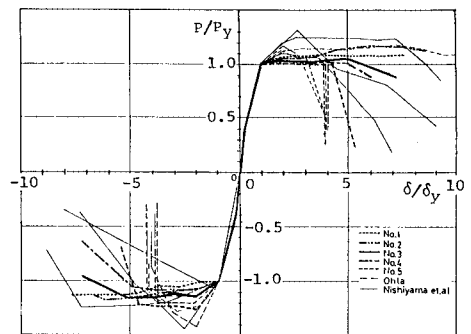


Fig.6 Envelopes of load-displacement relationship.

lopes of load-displacement relationship including the results of other research works^(10,15) is shown in Fig.6. The ordinate and abscissa in Fig.6 represents the load and the displacement normalized by yield load and yield displacement, respectively. In this figure, each test specimen has some differences in test condition and dimension, and the deformation capacity is clearly varied with the number of loading cycles.

(2) Accumulation of Absorbed Energy

Fig.7 shows the cumulative absorbed energy in column members for each loading amplitude. The number in the figure indicates the repetition of loading cycles. Cumulative absorbed energy was obtained by integrating the area at each loading step in load-displacement loop. As shown in the figure, the cumulative absorbed energy is remarkably different with the number of loading cycles. Based on the relation shown in Fig.7, the following second order regression curves were obtained for each number of loading cycles.

$$\begin{aligned}
 W_H &= 0.140 X^2 - 0.214 X + 0.168 & : N = 1 \\
 W_H &= 0.509 X^2 - 0.495 X + 0.026 & : N = 5 \dots\dots\dots (1) \\
 W_H &= 0.990 X^2 - 1.236 X + 0.303 & : N = 10
 \end{aligned}$$

where N = number of loading cycles, $X = n\delta_y$ ($n = 1, 2, 3, \dots$). The correlation coefficients of Eq.(1) between W_H and X was 0.98 or larger in the equations. These could be unified into the following single expression.

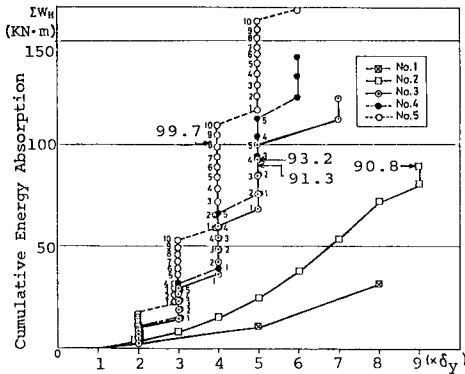


Fig.7 Cumulative energy-displacement relationship.

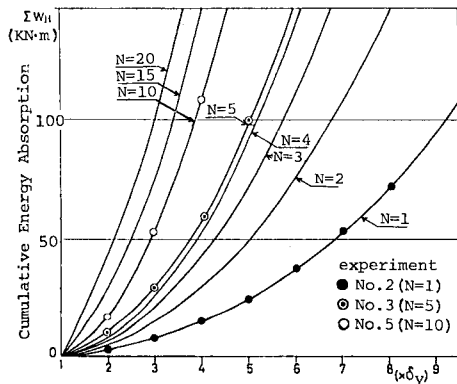


Fig.8 Effect of the number of loading cycles on energy absorption.

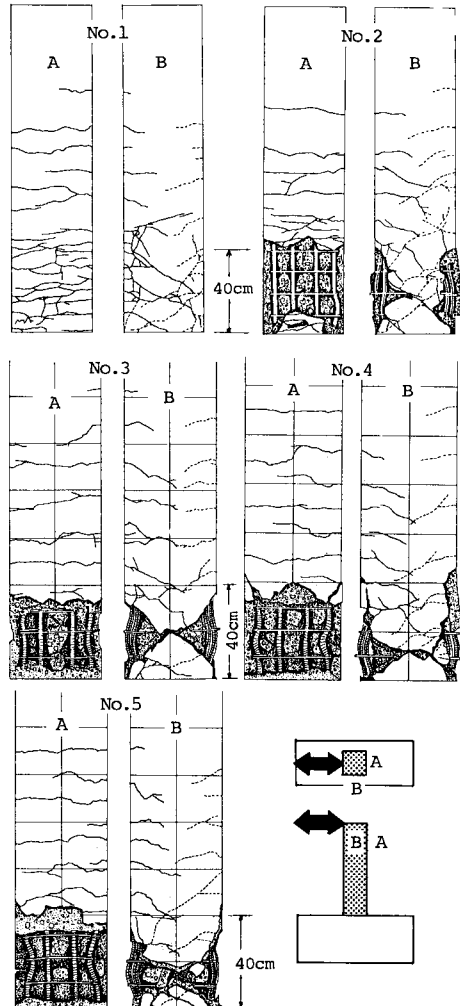


Fig.9 Final state of damage in columns.

$$W_H = (0.391 N^{\frac{1}{2}} - 0.287)X^2 - (0.473 N^{\frac{1}{2}} - 0.361)X + 0.01 N^2 - 0.096 N + 0.258 \dots\dots\dots (2)$$

where $N \geq 1$, $X \geq 2 \delta_y$.

Fig.8 shows the cumulative absorbed energy calculated by Eq.(2) in case of loading cycles $N=1, 2, 3, 4, 5, 10, 15$ and 20 . The cumulative absorbed energy by experiment shown in Fig.7 are also plotted by the marks $\bullet (N=1)$, $\odot (N=5)$ and $\circ (N=10)$, respectively. It shows that the cumulative absorbed energy is closely related to the loading amplitude $X (= n\delta_y)$ and the number of loading cycles N . According to Fig.8, when the number of loading cycles N is small, large loading amplitude X is needed to reach a certain cumulative absorbed energy. As the number of loading cycles is larger, the cumulative absorbed energy increases even if the amplitude is small. It means that the ductility of structural members is varied with the number of repeated loading cycles, when there exists the upper limit in cumulative absorbed energy.

(3) Final State of Damage in Specimens

The features at final state of damage in each specimen are shown in Fig.9. These are generally similar except the specimen No.1. The fracture of cover concrete and the buckling of axial reinforcing bars occurred within the range of 40 cm from the column foot in the specimens No.2-No.5. Though the fracture of cover concrete did not occur in the specimen No.1, the crack was concentrated within the range of 40-50 cm from the column foot as same as the other specimens. In the specimens No.2-No.5 the plastic hinges were observed on the surface parallel to the loading direction at the height of 20 cm from the foot.

(4) Distribution of Absorbed Energy

The distribution of absorbed energy in the member was examined to find the position of damage in column body. The column was divided into 9 zone for convenience. The cumulative absorbed energy in each zone was calculated by the measured curvature and bending moment. Fig.10 shows the relation

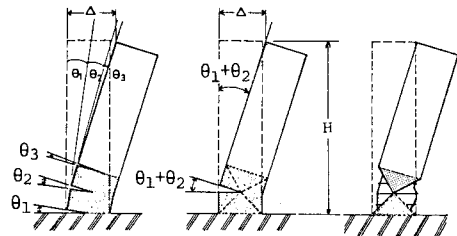


Fig.11 Simulated model for plastic deformation used in this study.

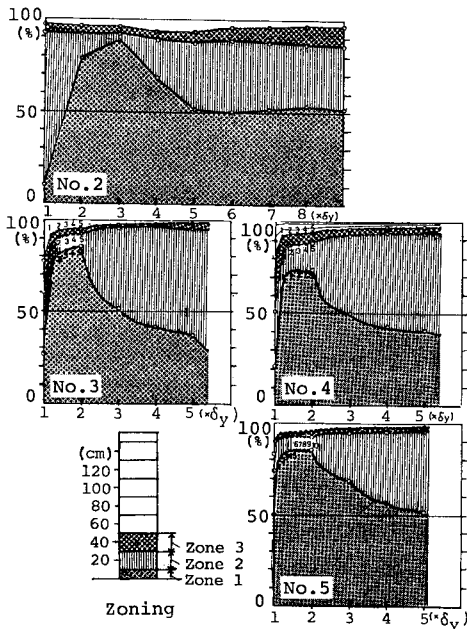


Fig.10 Distribution of energy absorption calculated from moment-curvature relationship.

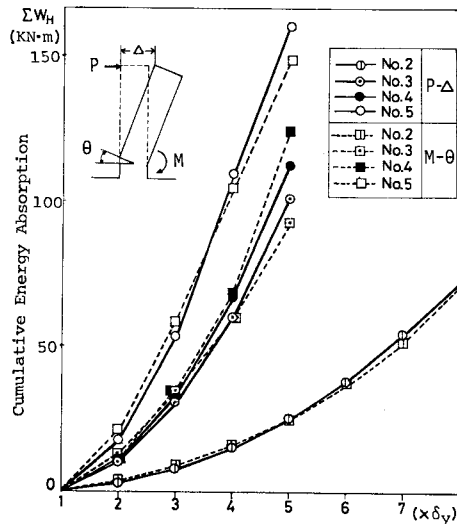


Fig.12 Cumulative energy absorption by load-displacement and moment-rotation relationship.

between the rate of absorbed energy distribution in each zone and the loading amplitude at each cycle. It shows that the absorbed energy distribution has same tendency in every cases. The rate of absorbed energy in Zone-1 increases abruptly at the amplitude $2 \delta_y$. The rate in Zone-2 increases after $2 \delta_y$ and approaches to the rate in Zone-1, as the loading amplitude becomes larger with the number of loading cycle. The rate in Zone-3 is small and shows almost constant values with no relation to loading amplitude and the number of loading cycles. The total rate of absorbed energy between Zone-1 and Zone-3 amounts to almost 95% in every specimens. It is noteworthy that the 90~95% of the whole absorbed energy is occupied from Zone-1 to Zone-2 and that the damage is concentrated in these sections. It corresponds well to the final state of damage as described in the previous section (3). The plastic region is regarded as the section from the column foot to the height of 40 cm (Zone-1 to Zone-3) based on the above consideration.

(5) Cumulative Energy Absorption by Moment-Rotation Relationship

It is regarded by the results of previous section (4) that the plastic region ranges from the column foot to the height of 40 cm and that the column rotation concentrates on the center of this region at the height of 20 cm from the foot. Since the behavior of column after yielding is considered almost due to the rotation of this plastic hinge region, the rotation angle of the plastic hinge (θ) can be regarded as the sum of θ_1 and θ_2 as shown in Fig.11. Fig.12 shows the comparison between the cumulative energy absorption calculated by the experimental results of the load (P)-displacement (Δ) relationship at the loading point and that of the moment (M)-rotation (θ) relationship calculated by internal energy in plastic region. The moment (M) is the one at the assumed section in which the plastic hinge was made. In Fig.12, the solid lines represent the cumulative energy absorption by P - Δ relationship, and the broken lines, by M - θ relationship. It should be noted in this figure that the cumulative energy absorption by M - θ relationship is almost equal to that by P - Δ relationship and that the assumption described above can be well suited. The plastic behavior of reinforced concrete columns after yielding can be investigated by using such a simplified concept that the plastic hinge is concentrated at the central cross section of plastic region.

(6) Energy Absorption Capacity

Fig.13 shows the general relation in the envelope of the load-displacement or the moment-rotation relationship of flexural reinforced concrete members. Though many definitions on the structural failure have been made, the structural failure defined in this study is the time when the member strength becomes smaller than its yield strength after it passes through its maximum strength. The amount of energy absorbed in the structural members up to this state is called in this study as the energy absorption capacity. The final displacement is the one that corresponds to the final state defined above in the load-displacement relationship, and the ductility factor is generally defined as the final displacement normalized by yield displacement. Fig.14 shows the relation among the maximum strength of the speci-

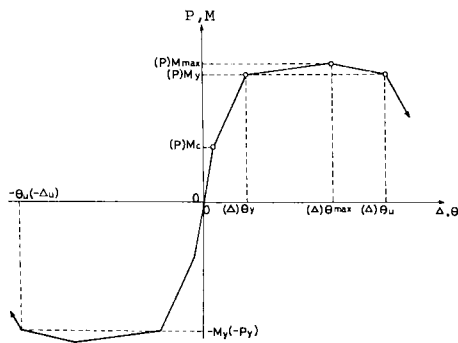


Fig.13 Idealized moment-rotation (load-displacement) relationship.

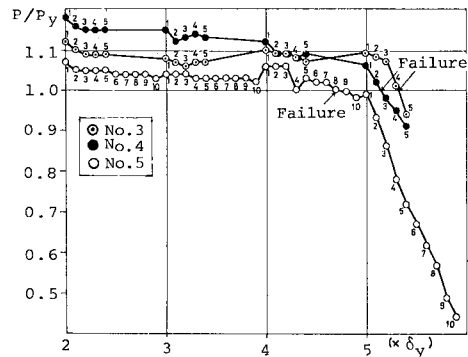
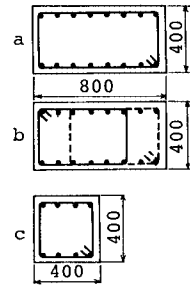


Fig.14 Variations of strength of column for repeated loading.

Table 5 Details of test specimens and their energy absorption capacity.

	Specimen	Ratio of Axial Reinforcement (%)	Interval of Ties (cm)	Ratio of Ties (%)	Type of Ties	Axial Unit Stress (MPa)	Energy Absorption Capacity (KN·m)			Loading Types
							①	②	③	
Ohta ¹⁵⁾	B	0.82	20	0.08	a	0.98	191.9	190.5	194.5	6 _y , 26 _y , 36 _y ... 10cycles each
	C		10	0.16	a		198.6			
	D		20	0.16	b		181.2			
Author	No. 2	0.82	10	0.32	c	0.98	90.8	93.8	95.8	L-2
	No. 3						93.2			L-3
	No. 4						91.3			L-4
	No. 5						99.7			



mens No.3-No5, the loading cycles and the loading amplitude. The ordinate represents the maximum load normalized by yield strength and the abscissa represents the loading amplitude. The number in the figure shows the repetition of loading cycles. In all specimens the maximum strength appears at the first cycle of $2\delta_y$ after yielding. The strength is gradually deteriorated after that with the increase of loading amplitude and the number of loading cycles. The point where the strength of members becomes lower than the yield strength (that is, the value lower than 1.0 in the figure) is at the fourth cycle of $5\delta_y$ in the specimen No.3, at the second cycle of $5\delta_y$ in the specimen No.4 and at the eighth cycle of $4\delta_y$ in the specimen No.5. Calculating the cumulative energy absorption by the load-displacement relationship up to these points, they were obtained as 93.2 KN·m, 91.3 KN·m and 99.7 KN·m in the specimens No.3, No.4 and No.5, respectively. These values are indicated also in Fig.7. It can be regarded almost equal to each other. It is noteworthy that there is not great difference in the cumulative energy absorption between the specimens No.3 and No.4 in spite of the difference in axial stress.

Ohta has reported experimental results on the strength and displacement capacity of various specimens in his research works¹⁵⁾. Since his experimental works have comparatively the same test condition and dimensions of specimens as in this study, energy absorption capacity was calculated by using these results and Muto's hysteresis model²⁶⁾. The results of calculation and the details of specimens were shown in Table 5. Though these specimens are somewhat different each other in the ratio of hoop ties and the type of ties, the value of energy absorption capacity are almost equal as shown in the column ① of Table 5. Comparing with the result of our study, the values of energy absorption capacity are almost twice, because the cross sectional area of the specimens by Ohta is just twice as much as that of ours. This fact indicates that the effects of axial unit stress and when the ratio of hoop ties on the energy absorption capacity are negligible when the axial unit stress is lower than 1.96 MPa and when the ratio of hoop ties ranges from 0.08 to 0.32%. It may be concluded from these facts that the members are equivalent in the energy absorption capacity when the shape of cross section, the ratio of axial reinforcing bars and shear-span ratio have the same condition.

(7) Quantitative Estimation of Energy Absorption Capacity

A column member of reinforced concrete structures in the condition of one fixed end such as reinforced concrete piers of bridges was the object for this study. Judging from the previous section (6), the energy absorption capacity of those structures is regarded as inherent and constant value in spite of loading cycle. If these energy absorption capacity could be obtained easily from the member constants, it would be very easily to estimate the earthquake resistance of structures by using energy concept.

Since the structural failure in this experiment was governed by the plastic hinge appeared at the specific cross section near fixed end, the energy absorption capacity was calculated quantitatively by making a model which reflects the column behavior in the experiment. If the behavior of the column is a perfectly rigid-plastic model under monotonic loading condition, the energy absorption capacity is simply calculated by the product of plastic strength and displacement capacity. The following equation described in Ref. 27) was adopted as the plastic strength.

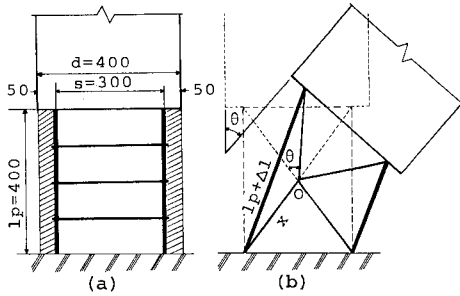


Fig.15 Mechanical model for plastic rotation capacity.

$M_p = 0.8 a_t \sigma_{sy} D + 0.5 ND(1 - N/bD\sigma_c) \dots\dots (3)$
 where $N \leq 0.4 bD\sigma_c$, a_t =cross sectional area of tensile reinforcement, σ_{sy} =yield strength of tensile reinforcement, N =axial load, b and D =width and depth of cross section, respectively. σ_c =compressive strength of concrete. Assuming the rotation of column is limited by geometric restriction due to the elongation of tensile reinforcing bars, such a simple model as shown in Fig.15 was used in the calculation. In the model, the cover concrete having the range of plastic region $l_p (=40 \text{ cm} = D)$ is ignored and the

column member rotates at the center of plastic region to its final state as shown in Fig.15(b). The ultimate rotation angle of the column θ_p in this state can be expressed as follows.

$\theta_p = 2 \{ \cos^{-1} l_p/2x - \cos^{-1}(l_p + \Delta l)/2x \} \cdot \pi/180 \text{ (rad.)} \dots\dots\dots (4)$

in which l_p =length of tensile reinforcing bars in plastic region, Δl =length of elongation in tensile reinforcing bars and $x = \sqrt{l_p^2 + s^2}/2$ (s =distance between both tension and compression reinforcement).

Substituting the experimental values of this study into Eq.(3) and (4), the plastic strength and the ultimate rotation angle are obtained. Taking $b = D = 40 \text{ cm}$, $\sigma_c = 24.8 \text{ MPa}$, $\sigma_{sy} = 362 \text{ MPa}$, $p_t = p_c = 0.82\%$, $l_p = 40 \text{ cm}$, $\Delta l = 7 \text{ cm}$ and $x = 25 \text{ cm}$, the plastic strength and the ultimate rotation angle yield to $M_p = 162.0 \text{ KN}\cdot\text{m}$ and $\theta_p = 0.591 \text{ rad.}$. Three reinforcing bars having the same length as the plastic region ($l_p = 40 \text{ cm}$) in the experiment were next tested to investigate the elongation capacity. Since all reinforcing bars in the test were rapidly broken after reaching to the maximum strength, the average elongation rate of 17.5% which corresponds to its maximum strength was used as the standard of elongation limit. Finally, the energy absorption capacity W_c of the specimens was obtained as $W_c = M_p \cdot \theta_p = 95.8 \text{ KN}\cdot\text{m}$.

Since the specimens given in Ref. 15) has the same depth in cross section and the same ratio of axial reinforcement as the present case, the ultimate rotation angle has the same value of $\theta_p = 0.591 \text{ rad.}$. The energy absorption capacity in this case was obtained as $W_c = 329.2(\text{KN}\cdot\text{m}) \times 0.591(\text{rad.}) = 194.5 \text{ KN}\cdot\text{m}$ by using Eq.(3) and (4). These two values were listed in the column ③ of Table 5. The column ① shows the experimental values of energy absorption capacity, and the column ② shows their average values. There is good coincidence between the experimental and analytical values. This may be due to the fact that the column behavior of reinforced concrete in flexural failure depends mainly on the behavior of axial reinforcing bars. It means that the energy absorption capacity of reinforced concrete structures could be estimated, if the cross sectional constants of members and the physical properties were given by the simple material tests of axial reinforcing bars and concrete. Once the energy absorption capacity is calculated by the above method, the structural safety under strong earthquake motion may be judged easily by comparing the input energy of structures imparted by earthquake with their energy absorption capacity.

4. CONCLUSION

The purpose of this study is to investigate the energy absorption capacity of reinforced concrete columns quantitatively. A series of five reinforced concrete columns were tested under four types of repeated loading. Based on the experiment, the effect of loading cycles on the energy absorption capacity was examined quantitatively. Though the test was limited in the number of specimens and condition, it suggested that the energy absorption capacity is a good index in earthquake resistant design when the seismic safety for structures are decided by their energy absorption capacity. The concluding remarks are expressed as follows.

(1) Though the ductility factor is influenced by the number of loading cycles, the energy absorption capacity is almost constant and is not affected by the number of loading cycles.

(2) The effects of axial unit stress and the ratio of hoop ties on the energy absorption capacity are negligible when the axial unit stress is within 0.98~1.96 MPa and the ratio of hoop ties ranges from 0.08 to 0.32%.

(3) If the cross sectional size of structural members and the properties of axial reinforcing bars and concrete were known, the energy absorption capacity of structural members can be estimated by using Eq.(3) and (4).

(4) Once the energy absorption capacity is calculated by the method presented in this paper, the structural safety under strong earthquake motion may be judged by the comparison between the input energy of structures imparted by earthquakes and their energy absorption capacity.

ACKNOWLEDGEMENTS

The authors would like to thank Mr. H. Kimura and Mr. M. Iidaka, Technical Staff of Institute of Engineering Mechanics in University of Tsukuba, and Miss K. Hoshikawa and Mr. T. Takeshima, Graduate Students of University of Tsukuba, for their cooperation in the experimental works. Special thanks are extended to Mr. N. Ueno, Undergraduate Student of University of Tsukuba, for his most helpful assistance. This research works was supported partly by the Grant-in-Aid for Scientific Research No. 57460136 from the Japanese Ministry of Education.

REFERENCES

- 1) Motoki, S., Matsushita, Y and Akino, T. : Experimental Study on Failure Mechanics of RC Columns-Part 1, Proc. of Annual Meeting of AIJ, pp.1431~1432, 1976.10 (in Japanese).
- 2) Ohno, K. et al. : Flexural Failure Features of RC Columns subjected to Dynamic Repeated Loading, Proc. of Annual Meeting of AIJ, pp.1443~1446, 1976.10 (in Japanese).
- 3) Arakawa, T. et al. : Estimation of Ductility of RC Columns subjected to Repeated Loading, Proc. of 3rd Annual Meeting of Concrete Engineering, pp.449~452, 1981 (in Japanese).
- 4) Ikeda, A. : Experiment of RC Columns under Repeated Loading in Plastic Region, Concrete Journal, Vol.8, No.12, pp.1~13, 1970.12 (in Japanese).
- 5) Kuromasa, S., Hayashi, S. and Nakano, T. : Study on Restoring Characteristics of RC Columns under Repeated Loading, Proc. of Annual Meeting of AIJ, pp.1393~1394, 1973 (in Japanese).
- 6) Shimazu, T. and Yamamoto, K. : On Repeated Characteristics of RC Columns, Proc. of Annual Meeting of AIJ, pp.791~792, 1971.11 (in Japanese).
- 7) Krawinkler, H. and Popov, E.P. : Hysteretic Behavior of Reinforced Concrete Rectangular and T-Beams, Proc. of 5th WCEE, pp.249~258, 1973.
- 8) Bertero, V.V., Bresler, B. and Liao, H. : Stiffness Degradation of Reinforced Concrete Members subjected to Cyclic Flexural Moments, EERC 69~12, 1973.
- 9) Brown, R.H. and Jirsa, J.O. : Reinforced Concrete Beams under Load Reversals, Journal of the ACI, Proc. V.68, No.5, pp.380~390, May 1971.
- 10) Nishiyama, H., Yasaku, H. and Akimoto, T. : Fundamental Tests on Strength of RC Bridge Piers subjected to High Stressing Repeated Loading, Proc. of 29th Annual Meeting of JSCE, pp.213~215, 1974.10 (in Japanese).
- 11) Akimoto, T. and Tomizawa, S. : Fundamental Tests on Strength of RC Bridge Piers subjected to High Stressing Repeated Loading (Part 2), Proc. of 31st Annual of JSCE, pp.156~157, 1976.10 (in Japanese).
- 12) Morihama, K., Ohta, M. and Takahashi, M. : Loading Tests of Reinforced Concrete Columns, Proc. of 35th Annual Meeting of JSCE, pp.99~100, 1980.10 (in Japanese).
- 13) Kawada, H. and Ohta, M. : Repeated Loading Tests of Modeled RC Bridge Piers, Proc. of 36th Annual Meeting of JSCE, pp.25~26, 1981.10 (in Japanese).
- 14) Yoshino, S., Ishibashi, T. and Suzuki, M. : Tests on Strength of RC Columns under Repeated Loading, Proc. of 36th Annual Meeting of JSCE, pp.27~28, 1981.10 (in Japanese).
- 15) Ohta, M. : A Study on Earthquake Resistant Design for Reinforced Concrete Bridge Piers of Single-Column Type, Report of the Public Works Research Institute, Ministry of Construction, Vol.153, March 1980 (in Japanese).
- 16) Ohno, T., Nishioka, T. and Fujino, Y. : Quantitative Estimation of Plastic Energy absorbed in Structures subjected to Seismic

- Excitation, Proc. of JSCE, No.333, pp.91~99, 1983.5 (in Japanese).
- 17) Ohno, T. and Nishioka, T. : Relation between the Hysteretic Characteristics of Structures and the Plastic Energy Dissipation under Earthquake Motion, Proc. of the 6th Earthquake Engineering Symposium, pp.1105~1112, 1982.12.
 - 18) Takeshima, T., Ohno, T. and Nishioka, T. : Linearized Estimation for Response of Structures Excited by Irregular Waves, Proc. of JSCE, No.344/1-1, pp.253~262, 1984.4 (in Japanese).
 - 19) Ohno, K., Shibata, T., Hattori, T. and Saito, Y. : Influence of Loading Hysteresis on Resistant Features of RC Beams (Part 3), Proc. of Annual Meeting of AIJ, pp.1277~1278, 1973 (in Japanese).
 - 20) Matsui, C. and Mitani, I. : Study on Elasto-Plastic Features of High Tensioned Steel Structures subjected to Vertical Load and Repeated Horizontal Load (Part 2), Proc. of Annual Meeting of AIJ, pp.1063~1064, 1973 (in Japanese).
 - 21) Yamada, Y., Iemura, H. and Nishimura, I. : Estimation of Seismic Resistance of Modeled RC Bridge Piers by Hysteretic Energy Dissipation, Proc. of 17th Earthquake Engineering Presentation, pp.231~234, 1983.7 (in Japanese).
 - 22) Akiyama, H. : Ultimate Earthquake Resistant Design of Structures, Tokyo University Press, 1980 (in Japanese).
 - 23) Suzuki, T. and Tamamatsu, K. : Experimental Study on Energy Absorption Capacity of Columns of Low Steel Structures (Part 1), Proc. of AIJ, No.279, pp.65~75, 1979 (in Japanese).
 - 24) Suzuki, T. and Tamamatsu, K. : Experimental Study on Energy Absorption Capacity of Columns of Low Steel Structures (Part 2), Proc. of AIJ, No.280, pp.19~24, 1979 (in Japanese).
 - 25) Okada, K., Koyanagi, W. and Rokugo, K. : Energy Dissipation in Flexural Failure Process of Reinforced Concrete Beams, Memoirs of the Faculty of Engr., Kyoto University, Vol. XLII PART 2, pp.209~227, 1980.
 - 26) Muto, K. : Dynamic Analysis of Structures, Maruzen Press, pp.173~174, 1977 (in Japanese).
 - 27) Architectural Institute of Japan : Calculating Standard of Reinforced Concrete Structures: Commentary, p.587, 1982 (in Japanese).

(Received October 28 1983)